Microstructure of Dental Amalgams Containing High and Low Copper Contents

MANOHAR L. MALHOTRA *and* KAMAL ASGAR

School of Dentistry, The University of Michigan, Ann Arbor, Michigan 48109, USA

Microstructure of commercial dental alloys and their amalgams were studied primarily by x-ray diffraction, optical metallography, scanning electron microscopy, and x-ray energy dispersive spectroscopy. X-ray diffraction revealed more phases than normally reported in these materials. Presence of new phases was discussed and their formation mechanism understood. Some phases having interacting 2θ° values with others were properly identified. Both new and conventional dental alloys and their amalgams, namely Tytin, Sybraloy, Dispersalloy, Kerr Spheraloy, Caulk Spherical, Shofu Spherical, and Caulk 20th Century Microcut were used to complete the investigation.

J Dent Res 56(12): 1481-1487, December 1977.

Dental alloy containing mostly silver and tin with some copper when reacted with mercury produced an amalgam which has been widely accepted as a restorative material for filling cavities. The simplified setting reaction has been mentioned as:

$$\gamma(\text{Ag, Sn, Cu}) + \text{Hg} \rightarrow \gamma_1\,(\text{Ag}_2\text{Hg}_3) + \gamma_2\,(\text{Sn}_{7\text{-}8}\text{Hg}) + \text{Cu}_6\text{Sn}_5 + \gamma(\text{Ag, Sn, Cu})\ \text{unreacted particles.}$$

In fact, the commercial dental alloy was not a single-phase alloy and contained more than one phase. This multiphase alloy on reaction with mercury produced an amalgam, a complicated material consisting of more than the above-listed phases. The goal of the present investigation was to systematically determine the microstructure in both original dental alloys and their corresponding amalgams. This was achieved using the modern technology of x-ray diffraction, optical and/or electron optical methods, and x-ray energy dispersive spectroscopy.

Received for publication August 30, 1976.
Accepted for publication February 22, 1977.
This investigation was presented in part at the 54th general meeting of the IADR, Miami Beach, Florida, March 1976.
This research was completely supported by a postdoctoral award to one of the authors (Dr. M. L. Malhotra) from the National Institute of Dental Research, National Institutes of Health, under Research Grant # 5 F32 DE-05029-02, Bethesda, Md.

Experimental Procedures

MATERIALS AND PREPARATION. — Table 1 shows the brand of the selected alloys, their manufacturers, batch numbers, mercury-to-alloy ratio, mechanical amalgamators used, trituration times, and the weights of the pestle in the specified capsules. Table 2 shows the approximate chemical composition and shape of these alloy particles. Cylindrical amalgam specimens were prepared following the parameters in Table 1 along with the ADA testing procedures.[1] The specimens were allowed to set at 37 ± 0.1 C for about one month prior to microstructure determination.

X-RAY DIFFRACTION ANALYSIS. — Both original alloys and their amalgam powders were analyzed separately using x-ray diffraction techniques. The x-ray machine used was a Phillip's (XRG-3000) x-ray generator with copper K_α radiation (λ = 1.54 Å) and a nickel filter. In order to obtain an accurate value for 2Θ°, the diffractometer scanning speed was adjusted to 1° per minute. The x-ray signal was recorded on a chart recorder calibrated for 1 inch equivalent to 1°. The 2Θ° values obtained from the diffraction peaks were converted into d-spacings (Å) using ASTM conversion tables.

POLISHING AND ETCHING TECHNIQUES. — A room temperature curing epoxy resin was used to mount specimens for polishing. The surface was rough polished first with four grades of emery papers; the finest grade was 4/0. Final polishing was achieved by using in order, 15 μm, 1 μm, and 0.05 μm dispersion alumina powder on a slowly revolving brass polishing lap covered with a billiard polishing cloth. The specimens were then washed thoroughly with distilled water and dried.

The polished specimens were etched by a chemical etchant developed by Allan et al.[2] When chemical solutions were used in order as

TABLE 1.
SELECTED DENTAL ALLOYS

Dental Alloy	Manufacturer	Batch Number	Mercury to Alloy Ratio (%)	Amalgamator Used	Trituration Time (Sec)	Weight of Pestle (gm)
Tytin (predispensed)	S.S. White Philadelphia, PA	17511	43.0	Capmaster	6	—
Sybraloy (predispensed)	Kerr Mfg. Co. Romulus, MI	1009751277	46.0	Caulk Vari-Mix II (M-2 setting)	10	0.206
Dispersalloy (predispensed)	Johnson & Johnson East Windsor, NJ	HRI 8137-002841	50.0	Caulk Vari-Mix II (M-2 setting)	12	0.689
Kerr Spheraloy (predispensed)	Kerr Mfg. Co. Romulus, MI	0805753169	48.5	Wig-L-Bug	20	0.185
Caulk Spherical (pellet)	L. D. Caulk Co. Milford, DE	1264-601010	46.2	Wig-L-Bug	20	0.594
Shofu spherical (powder)	Shofu Dental Corp., Menlo Park, CA.	297501	48.0	Wig-L-Bug	12	1.066
Caulk 20th Century Micro-cut (powder)	L. D. Caulk Co. Milford, DE	8J68	53.7	Caulk Vari-Mix II (M-2 setting)	14	0.594

All specimens were tested according to A.D.A. Specification.

TABLE 2.
APPROXIMATE CHEMICAL COMPOSITION OF DENTAL ALLOYS

Alloy	Major Elements* Ag (%)	Sn (%)	Cu (%)	Particle Shape
Tytin	60	27	13	sphere
Sybraloy	40	30	30	sphere
Dispersalloy	72	0	28	sphere (⅓ proportion)
	68-70	26-28	2-4	irregular (⅔ proportion)
Kerr Spheraloy	68-70	26-28	2-4	sphere
Caulk Spherical	68-70	26-28	2-4	sphere
Shofu Spherical	68-70	26-28	2-4	sphere
Caulk 20th Century Microcut	68-70	26-28	2-4	irregular

*Some alloys contain ≤ 1% zinc. However, zinc does not play any role in the microstructure determination of these alloys or in their corresponding amalgams and, therefore, is ignored.

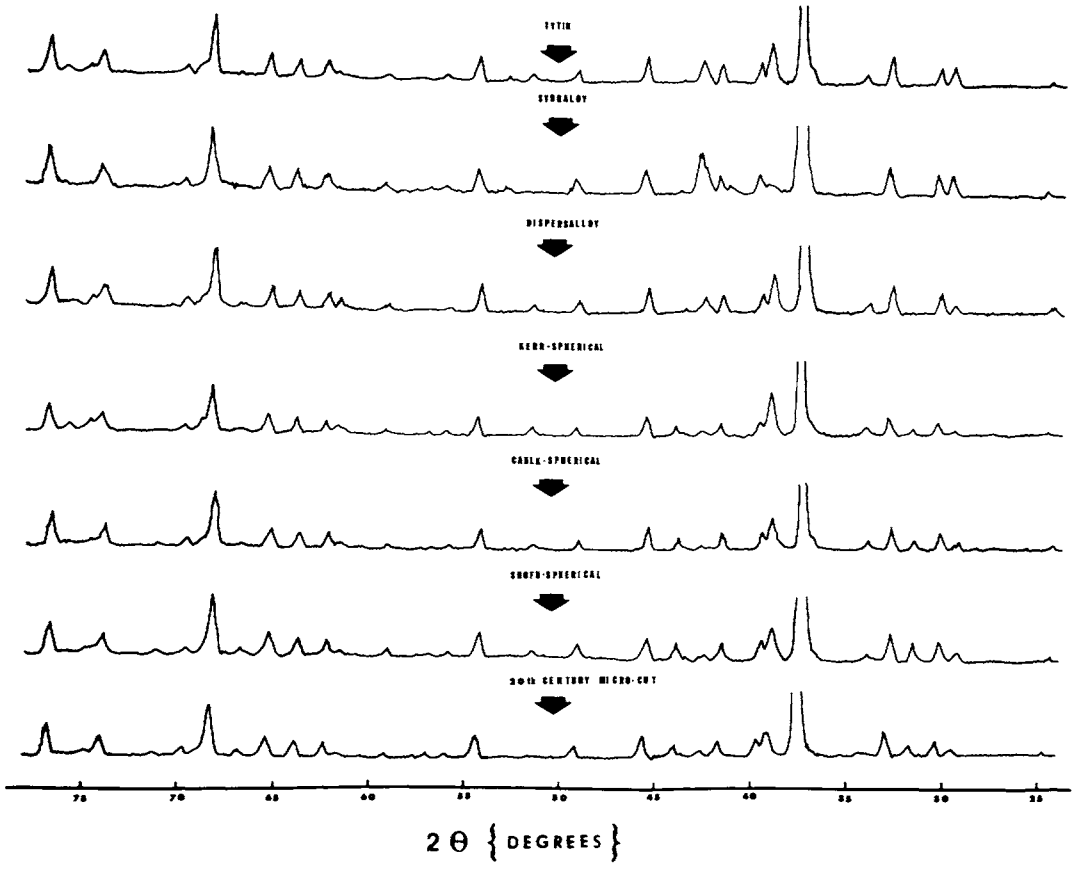

FIG 1. — X-ray diffraction patterns obtained from amalgams.

described by the authors, the specimen surface revealed all the required phases in dental amalgam.

METALLOGRAPHIC EXAMINATION. — The polished and etched specimens were examined on a Leitz Metallurgical microscope. Microstructure features were also obtained in the scanning electron microscope (Jeol Inc., JSM-U3). A Kevex Si (Li) x-ray energy dispersive spectrometer attached to the SEM was used to obtain x-ray energy spectra from the different elements present on the polished specimen surface. Identification of these elements qualitatively defined the presence of known phases on the specimen surface.

Results

Table 3 shows x-ray diffraction data obtained from original alloy powders. The $2\Theta°$ values obtained from the diffraction peaks, their relative intensities, and the identified phases with corresponding hkl indices are listed in the table. Figure 1 shows the complete x-ray diffraction patterns obtained from these amalgams. The phase analysis of these patterns is given in Table 4. Figure 2 shows the part of x-ray diffraction pattern over the important range of $2\Theta°$ values for γ_2 peaks for all amalgams studied.

Figure 3 shows an optical photomicrograph of a Shofu amalgam surface after being polished and etched by the procedures outlined in the previous section. Figure 4(a) shows a scanning electron photomicrograph of a typical enlarged area of a polished surface of Shofu amalgam. The areas marked "C" in Figure 4(a) were subjected to x-ray elemental analysis using the energy dispersive spectrometer, and the observed x-ray energy spectrum is shown in Figure 4(b).

Discussion

Prior to indexing of complicated diffraction patterns for amalgams containing multiple phases such as γ, γ_1, γ_2, Cu_3Sn, Cu_6Sn_5, Ag and/or Cu, it was decided to index relatively simple diffraction patterns from the original alloys containing γ, (Cu-Sn), Ag and/or Cu phases. This helped considerably in the further determination of microstructure in amalgams.

Table 3 shows a complete x-ray diffraction analysis of these selected original alloy powders. Most reactive element tin was completely utilized in forming γ and Cu_3Sn phases. Presence of Ag and/or Cu elements, which was obvious for Dispersalloy containing (Ag-Cu) eutectic phase, was never reported for other spherical alloys. These elements in small amounts might precipitate because of fast cooling rates produced in the atomization process.

Also, it was observed that Sybraloy containing 30% Cu and 30% Sn (Table 2) showed Cu_6Sn_5 phase which might be attributed to the high concentration of Cu and Sn elements present in this original alloy powder.

Figure 1 shows the complete x-ray diffraction patterns obtained from these amalgams. The phase analysis is given in Table 4. The unreacted γ and Cu_3Sn phases resulted from the original alloys. The γ_1 phase resulted from the two different reactions; (1) the reaction of mercury with silver part of Ag_3Sn (γ) phase and (2) the reaction of mercury with the silver element that

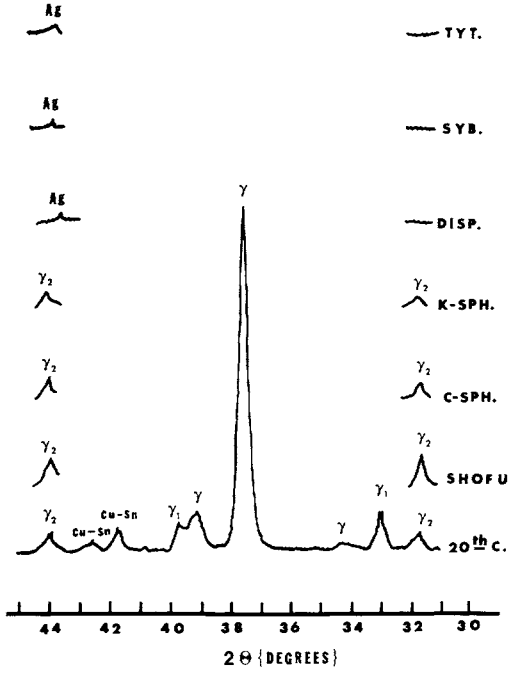

FIG 2. — Part of x-ray diffraction pattern over the range of 2Θ° values for γ_2 peaks in amalgams.

TABLE 3.
X-RAY DIFFRACTION ANALYSIS OF ALLOY POWDERS

Tytin 2Θ°	Sybra. 2Θ°	Disp. 2Θ°	K-Sph. 2Θ°	C-Sph. 2Θ°	S-Sph. 2Θ°	20th Cent. 2Θ°	Possible hkl	Probable hkl
—	31.6^W	—	—	—	—	—	Cu_6Sn_5 (101)	Cu_6Sn_5 (101)
34.0^M	33.9^M	34.0^M	33.7^M	34.5^M	34.4^M	34.3^M	γ (020,110)	γ (020,110)
36.9^M	36.8^M	37.0^M	36.7^M	37.5^M	37.2^M	37.3^M	γ (002)	γ (002)
—	—	37.6^M	—	37.9^M	—	—	Ag (111)	Ag (111)
38.9^S	38.8^S	39.0^S	38.7^S	39.5^S	39.4^S	39.3^S	γ (021,111)	γ (021,111)
40.9^W	40.8^M	—	—	—	—	41.2^W	Cu_3Sn (—)	Cu_3Sn (—)
42.5^M	42.4^S	42.5^M	42.3^W	42.9^W	42.6^W	42.9^W	Cu (111) Cu_3Sn (—) Cu_6Sn_5 (102,110)	Cu (111) Cu_3Sn (—)
—	—	43.8^M	43.0^W	44.0^W	—	—	Ag (200)	Ag (200)
51.4^M	51.3^M	51.5^M	51.2^M	51.9^M	51.9^M	51.8^M	γ (022,112)	γ (022,112)
56.6^W	56.5^M	—	—	—	—	—	Cu_3Sn (—) Cu_6Sn_5 (112)	Cu_3Sn (—)
61.6^M	61.6^M	61.6^M	61.3^M	62.0^M	61.9^M	61.9^M	γ (130,200) Cu_6Sn_5 (103,202)	γ (130,200)
—	—	64.0^W	63.0^W	64.3^W	—	—	Ag (220)	Ag (220)

Letters S, M, or W (S—strong, M—medium, W—Weak) on 2Θ°-values denote relative intensity of diffraction peaks.
hkl values for Cu_3Sn are not listed in ASTM tables.

was detected in the original alloys. During amalgamation, a large portion of Cu_3Sn phase from the original alloys containing this phase was converted into Cu_6Sn_5 phase.[3] This conversion of phases helped in a reduction of γ_2 phase in amalgams. Also, some diffraction peaks corresponding to other phases had $2\Theta°$ values which were close to the $2\Theta°$ values of γ_2 phase. To resolve this ambiguity, it was necessary to redraw part of the x-ray diffraction pattern over the range of $2\Theta°$ values for γ_2 peaks for all amalgams as shown in Figure 2. The following information was obtained from this figure:

(1) There were two diffraction peaks for γ_2 phase in the range of $2\Theta°$ values shown. It was found from standard tables that the diffraction peak for γ_2 phase at $2\Theta \sim 31.8°$ had higher intensity than the peak for γ_2 phase at $2\Theta \sim 44.0°$. The results indicated that Kerr Spheraloy, Caulk Spherical, Shofu Spherical, and Caulk 20th Century Microcut amalgams, classified as conventional amalgams, had both γ_2 peaks with intensities as expected. For Tytin, Sybraloy, and Dispersalloy amalgams, classified as new amalgams, the intense diffraction peak for γ_2 phase at $2\Theta \sim 31.8°$ was missing. A new weak diffraction peak at $2\Theta \sim 43.8°$ appeared in these amalgams. This new diffraction peak at $2\Theta \sim 43.8°$ was close to the diffraction peak for γ_2 phase at $2\Theta \sim 44.0°$. This might

TABLE 4.
X-RAY DIFFRACTION ANALYSIS OF AMALGAMS

Tytin 2θ°	Sybra. 2θ°	Disp. 2θ°	K-Sph. 2θ°	C-Sph. 2θ°	S-Sph. 2θ°	20th Cent. 2θ°	Rel. Inten.	Possible hkl	Probable hkl
24.6	24.8	24.4	—	24.5	24.5	—	W	γ_1 (220)	γ_1 (220)
29.7	29.7	29.5	29.7	29.5	29.3	29.5	M	Cu_6Sn_5 (101)	Cu_6Sn_5 (101)
30.4	30.5	30.2	30.5	30.4	30.2	30.4	M	γ_1 (222)	γ_1 (222)
—	—	—	31.9	31.8	31.8	31.8	M	γ_2 (100)	γ_2 (100)
32.9	33.0	32.8	33.1	32.9	32.8	33.0	M	γ_1 (321)	γ_1 (321)
34.2	—	34.0	34.3	34.2	34.0	34.3	W	γ (020,110)	γ (020,110)
37.6	37.7	37.4	37.7	37.6	37.4	37.6	S	γ (002), γ_1 (330,411), Ag (111)	γ (002), γ_1 (330,411)
39.2	39.4	39.0	39.2	39.1	39.0	39.2	M	γ (021,111)	γ (021,111)
39.8	39.8	39.5	39.8	39.6	39.5	39.7	M	γ_1 (420)	γ_1 (420)
41.8	41.9	41.6	41.8	41.7	41.6	41.7	M	γ_1 (332)	γ_1 (332)
42.8	42.8	42.5	42.8	42.8	42.6	42.6	M	Cu_3Sn (—), Cu (111), Cu_6Sn_5 (102,110)	Cu_6Sn_5 (102,110)
43.9	43.9	43.6	—	—	—	—	W	γ_1 (422), Ag (200)	Ag (200)
—	—	—	44.2	44.0	44.0	44.0	M	γ_2 (101)	γ_2 (101)
45.7	45.7	45.5	45.7	45.6	45.5	45.6	M	γ_1 (431,510)	γ_1 (431,510)
49.3	49.4	49.1	49.3	49.3	49.2	49.2	W	γ_1 (521)	γ_1 (521)
51.7	—	51.5	51.7	51.7	51.6	—	W	γ (022,112)	γ (022,112)
52.9	53.0	—	—	—	—	—	W	Cu_6Sn_5 (201)	Cu_6Sn_5 (201)
54.4	54.5	54.2	54.5	54.3	54.3	54.4	M	γ_1 (442,600)	γ_1 (442,600)
56.2	56.2	—	56.2	—	55.8	56.0	W	γ_1 (532,611), Cu_6Sn_5 (112)	Cu_6Sn_5 (112)
—	—	—	57.1	—	—	57.0	W	γ_2 (110)	γ_2 (110)
—	—	—	—	—	—	57.7	W	γ_1 (620)	γ_1 (620)
59.3	59.3	59.0	59.3	59.2	59.1	59.2	W	γ_1 (541), Cu_6Sn_5 (103)	γ_1 (541), Cu_6Sn_5 (103)
—	—	61.6	61.8	61.7	61.5	—	W	γ (130,200)	γ (130,200)
62.4	62.3	62.1	62.4	62.3	62.1	62.3	M	γ_1 (631), Cu_6Sn_5 (202)	γ_1 (631), Cu_6Sn_5 (202)
63.9	63.9	63.7	63.9	63.8	63.7	63.9	M	γ_1 (444), Ag (220)	γ_1 (444)
65.4	65.4	65.1	65.4	65.2	65.2	65.3	M	γ_1 (543,710), γ_2 (111)	γ_1 (543,710)

Letters S, M, or W (S—strong, M—medium, W—weak) denote relative intensity of diffraction peaks.
hkl values for Cu_3Sn are not listed in ASTM tables.

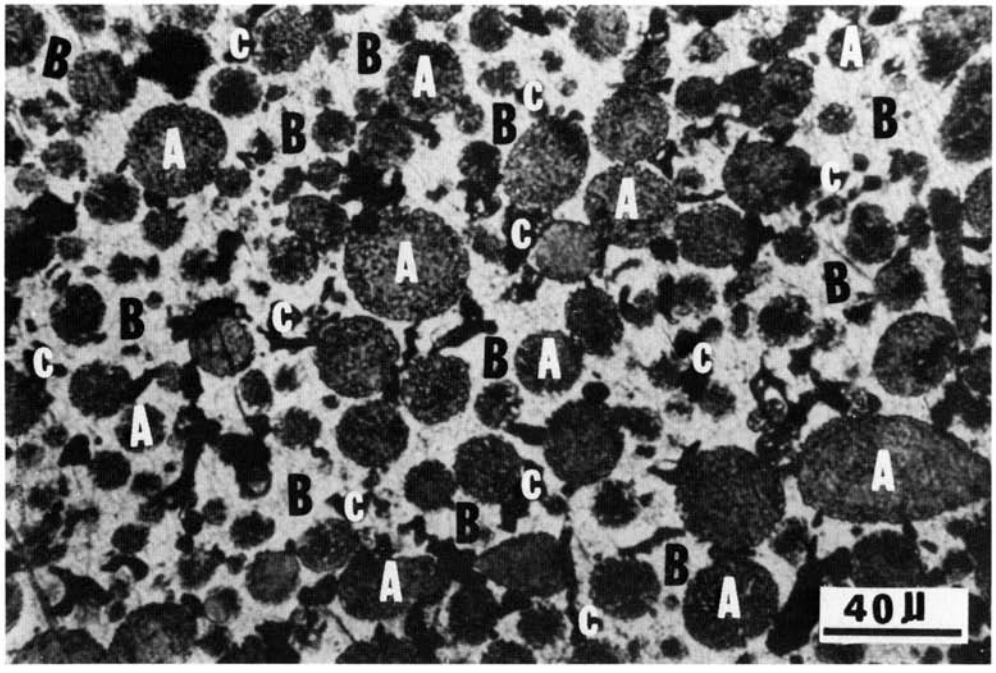

FIG 3. — A typical low magnification optical photomicrograph of a Shofu amalgam surface after being polished and etched.

lead to a wrong conclusion that this weak diffraction peak corresponded to γ_2 phase. In fact, this new weak diffraction peak was identified from Ag element. Thus, Tytin, Sybraloy, and Dispersalloy amalgams had no γ_2 phase in their microstructure.

(2) Careful investigation of the intensities of γ_2 peaks indicated that Shofu amalgam had more γ_2 phase among the γ_2-containing amalgams. This amalgam also showed peculiar mechanical properties, as reported.[4] This led us to further investigate this amalgam under the microscope. Figure 3 shows a low magnification optical photomicrograph of a Shofu amalgam surface after it was polished and etched according to procedures outlined earlier. The spherical particles marked "A" and the light matrix areas marked "B" were well-defined γ and γ_1 phases. Surprisingly, the dark areas marked "C" were scattered all over the surface. The dark areas "C" could correspond to either γ_2 phase or porosity normally observed in amalgams. Because of no contrast difference between γ_2 phase and porosity in the photomicrograph, it was then decided to determine the phase corresponding to dark "C" areas on the scanning electron microscope with an attached x-ray energy dispersive spectrometer. The specimen surface was again polished, thoroughly washed and dried. The polished surface was examined in the scanning electron microscope. Figure 4(a) shows a high magnification scanning electron photomicrograph of typical "C" areas on the specimen surface to be studied for energy dispersive x-ray analysis. Figure 4(b) shows the observed x-ray emission spectrum from the "C" areas of Figure 4(a). The spectrum indicated x-ray emission peaks for Al, Ag, Sn, and Hg elements. Aluminum appeared from the polishing alumina powder which was embedded in the specimen during the polishing process. Presence of weak Ag peak resulted from the penetration of the electron beam beneath the surface layers of the specimen. The remaining Hg and Sn elements corresponded to (Sn-Hg) phase, known as γ_2 ($Sn_{7-8}Hg$). This confirmed that the areas marked "C" in Figure 4(a), in fact, were γ_2 areas. Thus, Shofu amalgam had large γ_2 phase crystals as identified and scattered all over the surface (Fig 3). This was the reason that the diffraction pattern for Shofu amalgam showed intense γ_2 peaks comparing to other γ_2-containing amalgams.

Conclusion

The conclusion of the present study was made as follows:

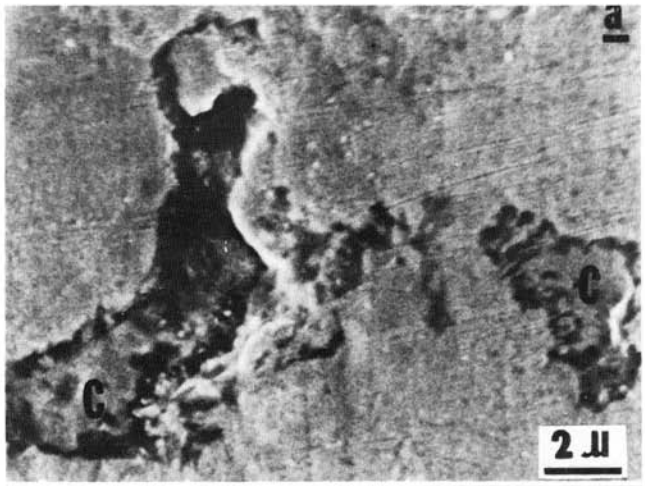

FIG 4(a). — Scanning electron photomicrograph of a polished Shofu amalgam surface; showing areas marked "C" to be studied for elemental analysis using energy dispersive x-ray spectrometer.

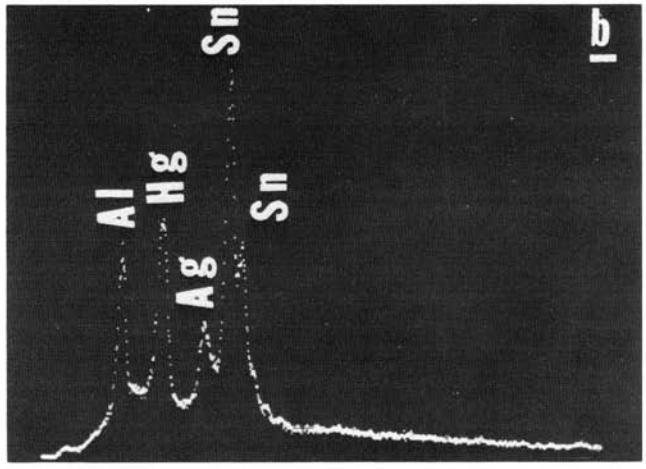

FIG 4(b). — X-ray emission spectrum observed from areas "C" in Figure 4(a).

(1) The amalgam contained both unreacted phases from the original alloy and the phases produced from the reaction of mercury with the original alloy. The unreacted phases from the original alloy were separately determined and then identified in the amalgam diffraction pattern. Then an effort was made to identify the remaining phases in the amalgam produced during amalgamation process. Also, interacting $2\Theta°$ values from different phases were carefully resolved.

(2) The silver element that was identified both in spherical alloys and their amalgams resulted from the fast cooling rates produced in atomization process.

(3) In an amalgam, the optical contrast produced for γ_2 and porosity was the same. Therefore, γ_2 phase was differentiated from porosity through the additional use of x-ray energy dispersive spectrometer.

(4) Shofu amalgam had large γ_2 crystals scattered all over the specimen.

(5) The present work demonstrated that Sybraloy amalgam, similar to Tytin and Dispersalloy amalgams, was free from γ_2 phase.

References

1. American Dental Association, *Guide to Dental Materials and Devices*, 7th ed, Chicago, Il, 1974-1975.
2. ALLAN, F. C.; ASGAR, K.; and PEYTON, F. A.: Microstructure of Dental Amalgam, *J Dent Res* 44:1002-1012, 1965.
3. MAHLER, D. B.; ADEY, J. D.; and EYSDEN, J. V.: Microprobe Analysis of a High Copper Amalgam Alloy, *DMG Microfilm, IADR Meeting*, Miami Beach, Fl, 1976.
4. MALHOTRA, M. L., and ASGAR, K.: Relationship Between Microstructure, Creep and Strength in Dental Amalgam, *DMG Microfilm, IADR Meeting*, Miami Beach, Fl, 1976.